

# $\mathbb{Z}_N$ Structure of Deconfinement Vacuum in $SU(N)$ Yang-Mills Theory: Nambu-Goldstone Mode in Large- $N$ Limit

Yuto Nakajima\*

*Faculty of Science, Kyoto University,  
Kitashirakawa-oiwake, Sakyo, Kyoto 606-8502, Japan*

Hideo Suganuma†

*Department of Physics, Graduate School of Science, Kyoto University,  
Kitashirakawa-oiwake, Sakyo, Kyoto 606-8502, Japan*

(Dated: April 18, 2023)

We investigate the structure of spontaneously broken  $\mathbb{Z}_N$  symmetry in the deconfinement vacuum in the  $SU(N)$  Yang-Mills theory using the Polyakov loop effective action. Firstly, we examine local fluctuations around a vacuum for finite  $N$  and show that the fluctuation in some direction becomes a Nambu-Goldstone mode in the large- $N$  limit. Secondly, we estimate the global vacuum-to-vacuum transition rate in a finite-volume domain of the quark-gluon plasma. Based on our estimation, we state that some threshold volume exists, a domain larger than which is stable, and vice versa. Identifying the threshold as the lower bound of a stable center domain volume, we find the typical volume scale of center domains quantitatively.

## I. INTRODUCTION AND SUMMARY

Quantum Chromodynamics (QCD) is currently considered the fundamental theory of strong interaction. Among various phenomena generated by QCD, the confinement of quarks is a crucial and fascinating non-perturbative aspect that characterizes physics at low energies. However, understanding the confinement remains a major challenge for QCD researchers, not only due to its non-Abelian properties but also because the perturbative theory is ineffective in this regime. Despite these theoretical difficulties, Wilson has introduced the lattice gauge theory [1], which has enabled us to treat confinement and achieved significant success to date.

In contrast, confinement is lost at high temperatures. Polyakov and Susskind have used the lattice gauge theory to demonstrate that a confined system gets deconfined at some temperature [2, 3]. The deconfined system, known as the quark-gluon plasma, is believed to have existed in the early universe and is created through relativistic heavy-ion collisions. Furthermore, the deconfinement phase transition is also an interesting subject of study in statistical mechanics. According to Yaffe and Svetitsky, the phase transition in QCD is first-order [4], and Ogilvie demonstrated that it is also first-order in the Yang-Mills theory with three or more colors [5].

The confinement in the Yang-Mills theory can be theoretically described using the Polyakov loop  $L$ , which have been first introduced by Polyakov [6]. The thermal average of the Polyakov loop  $\langle L \rangle$  corresponds to the partition function of a static quark  $F_q$ :  $\langle L \rangle \propto e^{-F_q/T}$ . If the thermal average is zero  $\langle L \rangle = 0$ , the confinement occurs. If it is non-zero  $\langle L \rangle \neq 0$ , the deconfinement is

signified. Therefore,  $\langle L \rangle$  serves as an order parameter for the confinement.

From a symmetry perspective, the deconfinement is interpreted as the spontaneous symmetry breaking (SSB) of the global  $\mathbb{Z}_N$  symmetry, which is the center of the gauge group  $SU(N)$ . The Yang-Mills action is invariant under the global  $\mathbb{Z}_N$  transformation, under which  $L$  undergoes a transformation  $L \mapsto zL$  ( $z \in \mathbb{Z}_N$ ). In the confinement phase, the  $\mathbb{Z}_N$  invariance of  $\langle L \rangle$  is respected, while in the deconfinement phase, the action retains the  $\mathbb{Z}_N$  symmetry but  $\langle L \rangle$  loses it. This is why the deconfinement vacuum has a nontrivial  $\mathbb{Z}_N$  structure that spontaneously breaks. This is the main topic of this paper.

In this paper, we aim to analyze the structure of the deconfinement vacuum using the Polyakov loop effective model in the  $SU(N)$  Yang-Mills theory. Svetitsky and Yaffe have derived a  $d$ -dimensional spin model that effectively describes the confinement from the  $(d+1)$ -dimensional Yang-Mills theory [7]. This spin model has the expected  $\mathbb{Z}_N$ -symmetry and belongs to the same universality class as the  $N$ -state Potts model [8]. The effective model is derived directly from the action of the Yang-Mills theory using the Migdal-Kadanoff renormalization group [5, 9] or the strong coupling expansion [10, 11]. Due to the strong coupling of the interactions in the quark-gluon plasma near the phase transition point, it is reasonable to use the strong coupling approximation in the analysis.

Analytical studies of the deconfinement vacua at finite  $N$  using the effective models have been conducted at the mean-field level in the literature such as the works by Matsuoka, Drouffe, and Ogilvie [5, 9, 12]. In this paper, we formulate an effective model incorporating non-uniformity and spatial fluctuations beyond the spatially uniform configuration. Moreover, we analyze the properties of the Polyakov loop by writing the explicit potential instead of using the distribution function of the Polyakov loop eigenvalues  $\rho(\theta)$ .

\* nakajima.yuto.62s@st.kyoto-u.ac.jp

† suganuma@scphys.kyoto-u.ac.jp

The Yang-Mills theory also has an interesting aspect, which is the large- $N$  limit. The large- $N$  limit not only provides deeper insights into QCD but also contains interesting academic aspects such as the AdS/CFT correspondence, the dominant contribution of planar diagrams [13], or the quarkyonic phase in high-density QCD [14]. Damgaard and Patk'os have exactly solved the Polyakov loop effective model in the large  $N$  limit [15]. Higher-order calculations by the character expansion have also been consistently performed by Bill'o et al. [16] While they assume  $N$  to be infinite from the stage of constructing the effective model, we take the large- $N$  limit of the results obtained from the effective model formulated at finite  $N$ . We restate the previous results in a more explicit form as described later.

Our first aim in this paper is to quantitatively evaluate the correlation length of the Polyakov loop for finite  $N$ . This theory has  $N$  different degenerate vacua at high temperature, reflecting the spontaneously broken  $\mathbb{Z}_N$  symmetry. One of these vacua is randomly chosen, and quantum and thermal effects cause local fluctuations around the vacuum. However, in the large- $N$  limit, we speculate that the degenerate vacua get connected to each other, and the global  $\mathbb{Z}_N$  symmetry becomes an approximately continuous  $U(1)$ . Then, the massive mode becomes massless. In fact, we show in Sec. III and IV that the mass of the fluctuation along some direction vanishes for the Potts model and the Yang-Mills theory, respectively. Although [15] has already pointed out the symmetry metamorphosis, we explicitly confirm it by utilizing a model with finite  $N$ .

Furthermore, in this paper, we evaluate the volume of center domains in the quark-gluon plasma. The plasma is created within a certain volume in experiments, and we expect the system to be divided into many small-volume center domains, as shown in Fig. 1. Each domain is characterized by its Polyakov loop configuration, which represents one of  $N$  degenerate vacua. Asakawa has studied the properties of the center domain wall [17]. Since the volume of each domain is finite, the global vacuum-to-vacuum transition rate does not vanish. We demonstrate quantitatively that the timescale for the configuration to remain around one vacuum changes abruptly before and after a certain volume: larger domains are stable, while smaller domains are not. Finally, we identify the volume threshold that determines its stability as the lower limit of the center domain volume.

In Section II, we summarize the general symmetry conversion from  $\mathbb{Z}_N$  to  $U(1)$ . In Sections III and IV, we formulate the effective action and demonstrate that some fluctuations become massless in the large- $N$  limit in the Potts model and the  $SU(N)$  Yang-Mills theory, respectively. In Section V, we consider the global vacuum-to-vacuum transition in the center domain with a finite volume and evaluate its lifetime and stability as a function of the number of colors and the volume. Section VI is devoted to the conclusion.

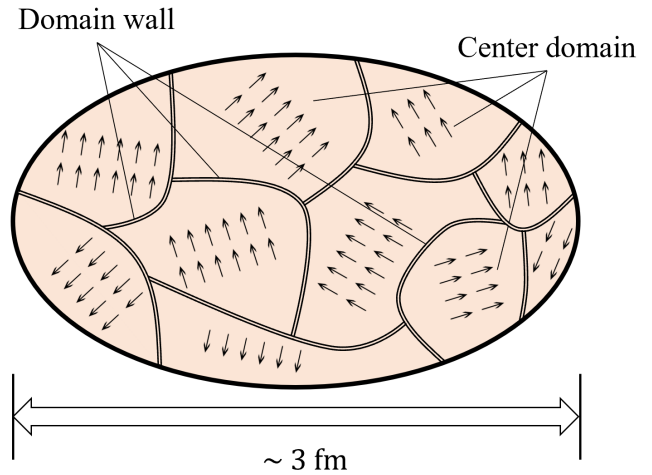


FIG. 1: The center domain of the quark-gluon plasma in the experimental situation. The arrows in the figure represent the phases of the vacuum expectation value of the Polyakov loop. Each domain, separated by the domain walls, is characterized by which vacuum the configuration is stabilized in.

## II. SYMMETRY CONVERSION

In this section, we summarize the fundamental properties of the symmetry conversion from  $\mathbb{Z}_N$  to  $U(1)$ . We consider an arbitrary action  $S[\varphi]$  involving a quantum field  $\varphi$  with global  $\mathbb{Z}_N$  symmetry:  $S[\varphi] = S[z\varphi]$  ( $z \in \mathbb{Z}_N$ ). We suppose that the symmetry is spontaneously broken in terms of its vacuum expectation value  $\langle \varphi \rangle \neq z\langle \varphi \rangle$ . In other words, we consider a theory with  $N$  different degenerate vacua. The problem is to determine whether the large- $N$  limit brings about qualitative changes in the symmetry.

It is essential to bear in mind that  $\mathbb{Z}_N$  is a discrete group. Nambu and Goldstone postulated that the spontaneous breaking of a global continuous symmetry results in the emergence of massless modes, the number of which corresponds to the number of broken degrees of freedom [18, 19]. In this sense, the spontaneous breaking of  $\mathbb{Z}_N$  symmetry does not necessarily result in the appearance of massless modes. However, massless modes can emerge in the large- $N$  limit because  $\mathbb{Z}_N$  symmetry is expected to become approximately continuous  $U(1)$  symmetry, as depicted in Fig. 2.

Although this is *a priori* speculation, we can demonstrate this type of conversion explicitly in some models. We achieve this by evaluating the correlation function of fluctuations in some direction and observing the behavior of the correlation length in the large- $N$  limit. The divergence of the correlation length (or the vanishing of the mode's mass) corresponds to the emergence of a Nambu-Goldstone mode. In the first part of this work, we demonstrate this conversion explicitly by using the  $\mathbb{Z}_N$  Potts model and  $SU(N)$  Yang-Mills theory.

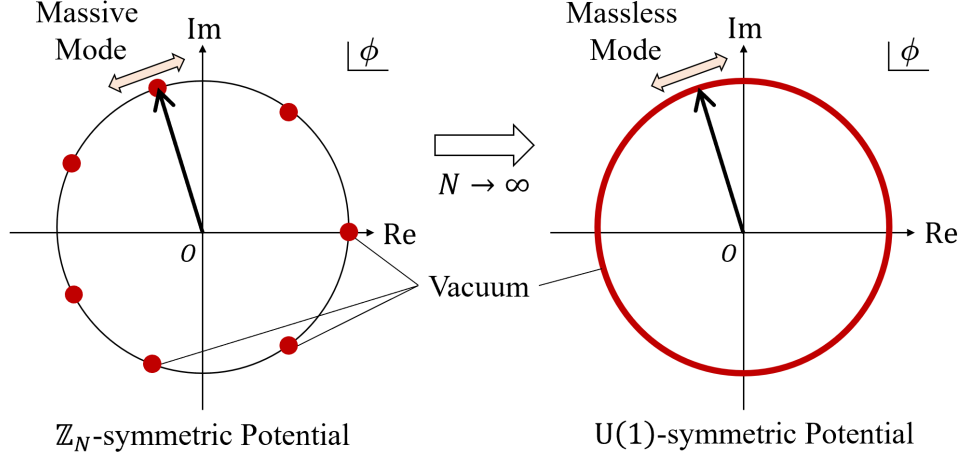


FIG. 2: In the large- $N$  limit, the  $\mathbb{Z}_N$ -symmetric potential is expected to become the  $U(1)$ -symmetric one, resulting in the conversion of  $\mathbb{Z}_N$  symmetry's SSB into that of a continuous symmetry. This leads to the generation of a massless mode in the angular direction.

### III. $\mathbb{Z}_N$ POTTS MODEL

In this section, we describe the above transformation in statistical mechanics using the Potts model [8, 20]. The model is defined by the Hamiltonian

$$H_{\text{spin}} = -J \sum_{\langle i,j \rangle} (S_i^* S_j + \text{c.c.}) \equiv -S^\dagger \hat{J} S, \quad (1)$$

where  $N_{\text{spin}}$  spin variables  $\{S_i\}$  take the values  $e^{i\frac{2\pi n}{N}} \in \mathbb{Z}_N$  ( $n = 1, 2, \dots, N$ ) and the sum  $\sum_{\langle i,j \rangle}$  is taken over all the nearest-neighbor spin variables. The Hermitian interaction coefficient matrix  $\hat{J}$  is defined as follows:

$$(\hat{J})_{ij} = \begin{cases} J (> 0) & (i \text{ and } j \text{ are the nearest neighbors}) \\ 0 & (\text{otherwise}) \end{cases} \quad (2)$$

It is obvious that (1) is invariant under the global  $\mathbb{Z}_N$  transformation:  $S_i \mapsto e^{i\frac{2\pi n}{N}} S_i$ .

In the following, we show that the large- $N$  limit generates a novel massless mode in the  $\mathbb{Z}_N$ -broken low-temperature region. Using the inverse temperature  $\beta$ , the partition function for this system reads

$$Z_{\text{spin}} = \text{Tr} e^{\beta S^\dagger \hat{J} S}. \quad (3)$$

To derive the effective action involving a dynamical quantum field, we introduce an auxiliary complex scalar field  $\phi = (\phi_1, \dots, \phi_{N_{\text{spin}}}) = (l_1 e^{i\theta_1/l_1}, l_2 e^{i\theta_2/l_2}, \dots, l_{N_{\text{spin}}} e^{i\theta_{N_{\text{spin}}}/l_{N_{\text{spin}}}})$  and convert (3) to the partition function with the dynamical variables. According to the method of Hubbard and Stratonovich, inserting the trivial path integral equation

$$\int \mathcal{D}\phi e^{-\beta(\phi^\dagger - S^\dagger \hat{J}) \hat{J}^{-1} (\phi - \hat{J} S)} = 1 \quad (4)$$

into (3), we obtain

$$\begin{aligned} Z_{\text{spin}} &= \int \mathcal{D}\phi e^{-\beta \phi^\dagger \hat{J}^{-1} \phi} \text{Tr} e^{\beta(S^\dagger \phi + \phi^\dagger S)} \\ &\equiv \int \mathcal{D}\phi \exp \left[ -\beta \phi^\dagger \hat{J}^{-1} \phi - \sum_i V(\phi_i) \right], \quad (5) \end{aligned}$$

where

$$V(\phi_i) \equiv -\ln \left( \sum_{n=1}^N e^{2\beta l_i \cos\left(\frac{2\pi n}{N} - \frac{\theta_i}{l_i}\right)} \right). \quad (6)$$

For simplicity, we omit the hat from  $\hat{J}$  from now on.

In the momentum space, the hopping term in (5) reads  $\sum_{i,j} \phi_i^* J_{ij}^{-1} \phi_j = N_{\text{spin}}^{-1/2} \sum_{\mathbf{k}} (1/\tilde{J}_{\mathbf{k}}) |\tilde{\phi}_{\mathbf{k}}|^2$ . Here  $\phi_i = N_{\text{spin}}^{-1/2} \sum_{\mathbf{k}} \tilde{\phi}_{\mathbf{k}} e^{i\mathbf{k} \cdot \mathbf{x}_i}$  and  $J_{ij} \equiv J_{\mathbf{r}} = N_{\text{spin}}^{-1/2} \sum_{\mathbf{k}} \tilde{J}_{\mathbf{k}} e^{i\mathbf{k} \cdot \mathbf{r}}$  ( $\mathbf{r} = \mathbf{x}_i - \mathbf{x}_j$ ). Taking the thermodynamical limit  $N_{\text{spin}} \rightarrow \infty$  and supposing the lattice spacing  $a$  is small, we approximately reduce the sum over discrete indices  $i$  to the integration over continuous variables<sup>1</sup>:

$$\begin{aligned} &N_{\text{spin}}^{-1/2} \sum_{\mathbf{k}} \frac{1}{\tilde{J}_{\mathbf{k}}} |\tilde{\phi}_{\mathbf{k}}|^2 \\ &\simeq \int \frac{d^3 \mathbf{k}}{(2\pi)^3} \frac{1}{\tilde{J}(\mathbf{k})} |\tilde{\phi}(\mathbf{k})|^2 \\ &\simeq \frac{1}{6Ja^3} \int \frac{d^3 \mathbf{k}}{(2\pi)^3} \left( 1 + \frac{a^2}{6} \mathbf{k}^2 \right) |\tilde{\phi}(\mathbf{k})|^2. \quad (7) \end{aligned}$$

<sup>1</sup> Here we define  $\phi(\mathbf{x}) \equiv \phi_i$ ,  $\tilde{\phi}(\mathbf{k}) = a^3 N_{\text{spin}}^{1/2} \tilde{\phi}_{\mathbf{k}}$ ,  $J(\mathbf{r}) = J_{\mathbf{r}} = J_{ij}$ ,  $\tilde{J}(\mathbf{k}) = a^3 N_{\text{spin}}^{1/2} \tilde{J}_{\mathbf{k}}$ . The coefficients reproduce the Fourier transformation of the continuous variables, that is,  $\phi(\mathbf{x}) = \int \frac{d^3 \mathbf{p}}{(2\pi)^3} \tilde{\phi}(\mathbf{k}) e^{i\mathbf{k} \cdot \mathbf{x}}$  or  $\tilde{\phi}(\mathbf{k}) = \int d^3 \mathbf{x} \phi(\mathbf{x}) e^{-i\mathbf{k} \cdot \mathbf{x}}$ . Using the matrix product  $\sum_j J_{ij} J_{jk}^{-1} = \delta_{ik}$  yields  $(\tilde{J}^{-1})_{\mathbf{k}} = (N \tilde{J}_{\mathbf{k}})^{-1}$ .

In the third line, we expand  $\tilde{J}(\mathbf{k})$  in terms of  $\mathbf{k}$  and ignore the higher-order terms to focus on the infrared region  $|\mathbf{k}| \ll a^{-1}$  because now we are interested in the long-range correlations in the large- $N$  limit.

Since the nearest-neighbor interaction yields  $J(\mathbf{r}) = Ja^3 \sum_{i=1}^6 \delta^3(\mathbf{r} - \mathbf{a}_i)$ , we obtain  $\tilde{J}(\mathbf{k}) = Ja^3 \sum_{i=1}^6 e^{-i\mathbf{k}\cdot\mathbf{a}_i} = Ja^3(6 - a^2\mathbf{k}^2) + \mathcal{O}(\mathbf{k}^4)$ .  $\{\mathbf{a}_i\}$  denotes the nearest grid points from the origin.

Combining (5), (6), and (7), we obtain the three-dimensional action for the complex scalar field  $\phi$ :

$$S_{\text{spin}}[\phi(\mathbf{x})] = \frac{\beta}{36Ja} \int d^3\mathbf{x} \left( |\nabla\phi(\mathbf{x})|^2 + \frac{6}{a^2} |\phi(\mathbf{x})|^2 + \frac{36J}{a^2\beta} V(\phi(\mathbf{x})) \right). \quad (8)$$

The partition function reads  $Z_{\text{spin}} = \int \mathcal{D}\phi \exp[-S_{\text{spin}}[\phi(\mathbf{x})]]$ . In the low-temperature region, the  $\mathbb{Z}_N$  symmetry is spontaneously broken, i.e. the vacuum expectation value is nonzero:  $\langle \phi \rangle \neq 0$ .

We consider fluctuations of  $\phi(\mathbf{x}) = l(\mathbf{x})e^{i\theta(\mathbf{x})/l(\mathbf{x})}$  around a vacuum. To obtain the mass of the fluctuation along the  $\theta$  direction, we freeze the  $l$  direction i.e. substitute  $\phi(\mathbf{x}) = l_0 e^{i\theta(\mathbf{x})/l_0}$  ( $l_0 : \text{const.}$ ) into (8) to get

$$\begin{aligned} S_{\text{spin}} &\simeq \frac{\beta}{36Ja} \int d^3\mathbf{x} \left( \frac{1}{2} (\nabla\theta)^2 + \frac{9J}{a^2\beta} V''(l_0)\theta^2 \right) \\ &\equiv \frac{\beta}{36Ja} \int d^3\mathbf{x} \left( \frac{1}{2} (\nabla\theta)^2 + \frac{m_{\text{spin}}^2}{2} \theta^2 \right), \end{aligned} \quad (9)$$

extracting the trivial constant. Here we expand (6) up to the second-order in terms of  $\theta$  considering that the  $\theta$  fluctuation is small:  $V(l_0 e^{i\theta(\mathbf{x})/l_0}) = V(l_0) + \frac{1}{2} V''(l_0)\theta^2 + \mathcal{O}(\theta^4)$ . The invariance under the transformation  $\theta \mapsto -\theta$  prohibits the odd-order terms.

Thus, the correlation function of  $\theta$  reads

$$\begin{aligned} \langle \theta(\mathbf{x})\theta(0) \rangle &= \frac{\int \mathcal{D}\theta \theta(\mathbf{x}) \theta(0) e^{-S_{\text{spin}}}}{\int \mathcal{D}\theta e^{-S_{\text{spin}}}} \\ &\propto \frac{1}{|\mathbf{x}|} e^{-m_{\text{spin}}|\mathbf{x}|}. \end{aligned} \quad (10)$$

The explicit formula

$$\begin{aligned} \lim_{N \rightarrow \infty} \frac{\partial^2}{\partial\theta^2} \ln \left( \sum_{n=1}^N e^{2\beta l_0 \cos\left(\frac{2\pi n}{N} - \frac{\theta}{l_0}\right)} \right) \\ = \frac{\partial^2}{\partial\theta^2} \ln \left( \frac{1}{2\pi} \int_0^{2\pi} d\varphi e^{2\beta l_0 \cos\left(\varphi - \frac{\theta}{l_0}\right)} \right) = 0 \end{aligned} \quad (11)$$

is followed by that  $m_{\text{spin}}$  goes to zero in the large- $N$  limit, which suggests that in the limit  $\langle \theta(\mathbf{x})\theta(0) \rangle \propto 1/|\mathbf{x}|$ . This clearly indicates the emergence of the long-range correlation or the Nambu-Goldstone mode.

#### IV. SU(N) YANG-MILLS THEORY

In this section, we move to the SU( $N$ ) Yang-Mills theory at finite temperature. First of all, we briefly review the gauge theory on the lattice and formulation of the effective theory in the problem. Without any dynamical fermions, the partition function is given by

$$Z_{\text{YM}} = \int \mathcal{D}U e^{-S_{\text{YM}}[U]}, \quad (12)$$

where  $S_{\text{YM}}[U]$  is the Wilsonian action [1]:

$$S_{\text{YM}}[U] = -\frac{1}{2g^2} \sum_{\square} \text{Re Tr} \square_{\mu\nu}(n). \quad (13)$$

The variables  $U_{\mu}(n)$  and  $\square_{\mu\nu}(n)$  represent the link variable and plaquette, respectively. Specifically,  $U_{\mu}(n)$  is defined as  $\exp[-iagA_{\mu}(n)] \in \text{SU}(N)$ , while  $\square_{\mu\nu}(n)$  is obtained from four adjacent link variables  $U_{\mu}(n)U_{\nu}(n+\hat{\mu})U_{\mu}^{\dagger}(n+\hat{\nu})U_{\nu}^{\dagger}(n)$ . The Haar measure on SU( $N$ ) is represented by  $\mathcal{D}U$ , which is the product of the measure for all link variables  $U_{\mu}(n)$ . The sum over all possible plaquettes is denoted by  $\sum_{\square}$ . The constant  $g$  represents the Yang-Mills coupling. To account for the finite temperature in the system, we enforce periodic boundary conditions along the imaginary time  $\tau$  direction, with the period of inverse temperature  $\beta = aN_{\tau}$ . This is done by setting  $U_{\mu}(1, i) = U_{\mu}(N_{\tau} + 1, i)$ . Here,  $N_{\tau}$  represents the number of links along the imaginary time  $\tau$  direction.

In the Yang-Mills theory at finite temperature, the confinement phase transition is described by the thermal average of the Polyakov loop

$$L_i = \prod_{i_{\tau}=1}^{N_{\tau}} U_{\tau}(i_{\tau}, i) \in \text{SU}(N) \quad (14)$$

as an order parameter. An effective action, whose dynamical variable is the Polyakov loop, should be invariant under the global  $\mathbb{Z}_N$  transformation:  $L_i \rightarrow zL_i$  ( $z \in \mathbb{Z}_N$ ) and we expect the symmetry is spontaneously broken at high temperature.

The effective action is naively formulated as

$$\begin{aligned} Z_{\text{YM}} &= \int \mathcal{D}U e^{-S_{\text{YM}}[U]} \\ &= \int \mathcal{D}U e^{-S_{\text{YM}}[U]} \int \mathcal{D}\phi_i \delta \left[ \phi_i - \frac{1}{N} \text{Tr}(L_i) \right] \\ &\equiv \int \mathcal{D}\phi e^{-S_{\text{eff}}[\phi]}. \end{aligned} \quad (15)$$

Although it is easy to see the structure of the symmetry, it is not clear how to calculate path integrals with such constraint conditions in (15). Therefore, we need to find another method such as the Hubbard-Stratonovich transformation in (5) to obtain the concrete form of effective action.

<sup>2</sup> Note that  $\bullet'$  denotes the differentiation with respect to  $\theta$ .

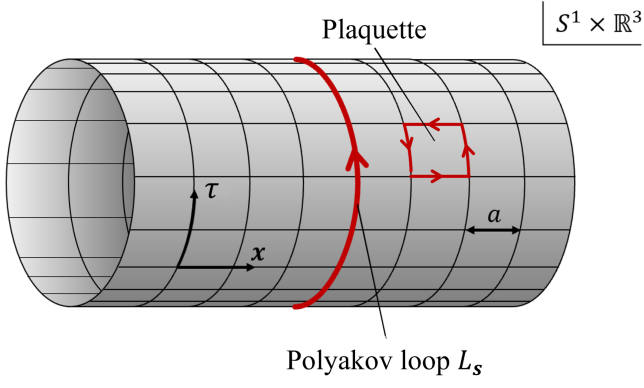


FIG. 3: The Polyakov loop and the plaquette on the lattice are shown in the figure. At finite temperature, the Euclidean spacetime is periodic in the imaginary time  $\tau$  direction. After integrating out all the space-like link variables, the action depends only on the Polyakov loops under the strong coupling approximation. The thermal expectation value of the loop serves as the order parameter for the deconfinement transition.

### A. Formulation

The Polyakov loop effective action is obtained from (13). This derivation is based on the Migdal-Kadanoff renormalization group [5, 9] or the strong coupling expansion [10, 11]. From the perspective of strong coupling approximation, we integrate out all the space-like link variables and obtain

$$Z_{\text{YM}} \simeq \int \left( \prod_{i_\tau=1}^{N_\tau} \prod_i dU_\tau(i_\tau, i) \right) \exp \left[ \left( \frac{1}{g^2 N} \right)^{N_\tau} \sum_{\langle i, j \rangle} \text{Tr}(L_i^\dagger) \text{Tr}(L_j) \right] \quad (16)$$

as an approximation up to the leading order. Here we fix the temporal gauge, where all the time-like link variables  $U_\tau(i_\tau, i)$  are set to 1 except for  $i_\tau = 1$  case, i.e. we set

$$U_\tau(i_\tau, i) = \begin{cases} U_\tau(i_\tau, i) & (i_\tau = 1) \\ 1 & (i_\tau = 2, 3, \dots, N_\tau) \end{cases} \quad (17)$$

Under the gauge, we can conduct  $\int dU_\tau(2, i) \dots dU_\tau(N_\tau, i)$  trivially. We replace  $dU_\tau(1, i)$  with  $dL_i$  and  $\prod_i dL_i$  with  $DL$  for later convenience. Fixing the string tension at zero temperature  $\sigma = a^{-2} \ln(g^2 N)$ , we can write down the partition function

$$Z_{\text{YM}} = \int DL \exp \left[ e^{-\beta\sigma a} \sum_{\langle i, j \rangle} \text{Tr}(L_i^\dagger) \text{Tr}(L_j) \right]. \quad (18)$$

The sum  $\sum_{\langle i, j \rangle}$  is taken over all the nearest-neighbor Polyakov loops. When the invariant integral over the group is converted to the one over the traced Polyakov

loops  $\phi_i = N^{-1} \text{Tr}(L_i)$  by  $dL_i = d\phi_i \mathcal{H}^{(N)}(\phi_i)$ , the partition function reads

$$Z_{\text{YM}} = \int \mathcal{D}\phi \exp \left[ N^2 e^{-\beta\sigma a} \sum_{\langle i, j \rangle} \phi_i^* \phi_j + \sum_i \ln \mathcal{H}^{(N)}(\phi_i) \right] \\ \equiv \int \mathcal{D}\phi \exp \left[ -\phi^\dagger \hat{\mathcal{J}}^{-1} \phi + \sum_i \ln \mathcal{H}^{(N)}(\phi_i) \right], \quad (19)$$

where  $\phi = (\phi_1, \phi_2, \dots)$  and  $\hat{\mathcal{J}}^{-1}$  (we write just  $\mathcal{J}^{-1}$  for simplicity from now on) denotes the coefficient matrix. (19) takes the same form as (5). Through the same analysis as (7), we obtain <sup>3</sup>

$$\sum_{i, j} \phi_i^* \hat{\mathcal{J}}_{ij}^{-1} \phi_j \\ = N_{\text{lat}}^{-1/2} \sum_{\mathbf{k}} \frac{1}{\tilde{\mathcal{J}}_{\mathbf{k}}} |\tilde{\phi}_{\mathbf{k}}|^2 \\ \simeq -\frac{6N^2 e^{-\beta\sigma a}}{a^3} \int \frac{d^3 \mathbf{k}}{(2\pi)^3} \left( 1 - \frac{a^2}{6} \mathbf{k}^2 \right) |\phi(\mathbf{k})|^2. \quad (20)$$

Such coarse graining of the short-wavelength modes leads to the effective action for the Polyakov loop:

$$S_{\text{YM}}[\phi(\mathbf{x})] = C \int d^3 \mathbf{x} \left( |\nabla \phi(\mathbf{x})|^2 - \frac{6}{a^2} |\phi(\mathbf{x})|^2 - \frac{e^{\beta\sigma a}}{N^2 a^2} \ln \mathcal{H}^{(N)}(\phi(\mathbf{x})) \right). \quad (21)$$

The partition function reads  $Z_{\text{YM}} = \int \mathcal{D}\phi e^{-S_{\text{YM}}[\phi(\mathbf{x})]}$  and  $C \equiv a^{-1} N^2 e^{-\beta\sigma a}$ .

Although we construct this model on a lattice, we treat it as a continuous field model because we focus on the emergence of long-range correlations, specifically in the infrared region where  $|\mathbf{k}| \ll a^{-1}$ . We assume that the lattice spacing is small enough compared to the typical wavelength of such correlations.

Next, we construct one of the important ingredients in (21), the Jacobian  $\mathcal{H}^{(N)}(\phi)$ . In the  $N = 2$  and  $N = 3$  case, it is known that the  $\text{SU}(2)$  Jacobian  $\mathcal{H}^{(2)}$  and  $\text{SU}(3)$  Jacobian  $\mathcal{H}^{(3)}$  reads

$$\mathcal{H}^{(2)}(\phi) = 1 - \phi^2 \quad (22)$$

$$\mathcal{H}^{(3)}(\phi) = 1 - 6|\phi|^2 - 3|\phi|^4 + 8\text{Re} \phi^3, \quad (23)$$

respectively as shown in Fig. 4 [21]. The  $\text{SU}(N)$  Jacobian is expectedly invariant under the global  $\mathbb{Z}_N$  transformation:  $\phi \mapsto e^{i\frac{2\pi n}{N}} \phi$ .

<sup>3</sup> Since the nearest-neighbor interaction yields  $\mathcal{J}^{-1}(\mathbf{r}) = -N^2 a^3 e^{-\beta\sigma a} \sum_{i=1}^6 \delta^3(\mathbf{r} - \mathbf{a}_i)$ , we obtain  $\tilde{\mathcal{J}}^{-1}(\mathbf{k}) = -N^2 a^3 e^{-\beta\sigma a} \sum_{i=1}^6 e^{-i\mathbf{k} \cdot \mathbf{a}_i} = -N^2 a^3 e^{-\beta\sigma a} (6 - a^2 \mathbf{k}^2) + \mathcal{O}(\mathbf{k}^4)$ . Using  $(\tilde{\mathcal{J}}^{-1})_{\mathbf{k}} = 1/N_{\text{lat}} \tilde{\mathcal{J}}_{\mathbf{k}}$  yielded from the matrix product  $\sum_j \mathcal{J}_{ij} \mathcal{J}_{jk}^{-1} = \delta_{ik}$  and  $\tilde{\mathcal{J}}(\mathbf{k}) = a^3 N_{\text{lat}}^{1/2} \tilde{\mathcal{J}}_{\mathbf{k}}$ , we can derive  $1/\tilde{\mathcal{J}}(\mathbf{k}) = a^{-6} \tilde{\mathcal{J}}^{-1}(\mathbf{k}) \simeq -6a^{-3} N^2 e^{-\beta\sigma a} (1 - a^2 \mathbf{k}^2/6)$ .

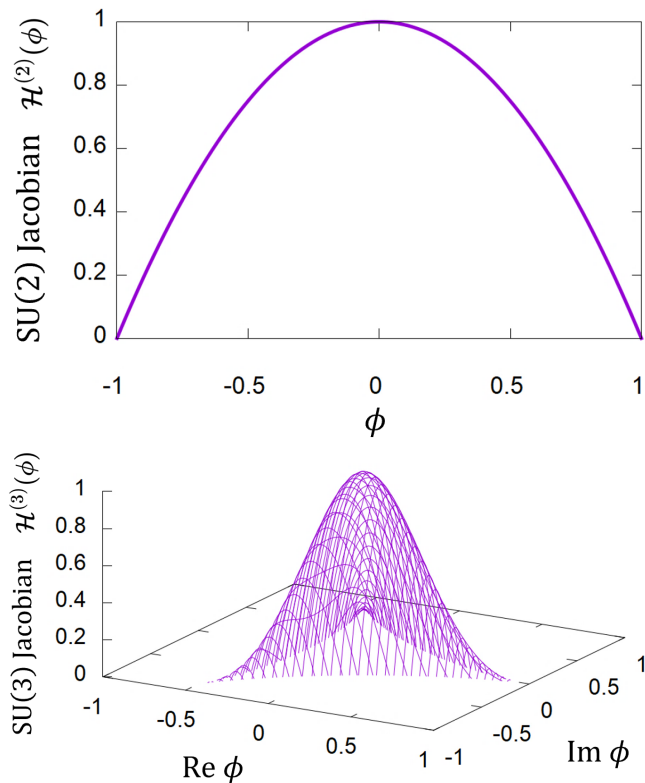


FIG. 4: The figures show the  $SU(N)$  Jacobian for  $N = 2$  (upper panel) and  $N = 3$  (lower panel) as a function of the traced Polyakov loop  $\phi$ . In the case of  $N = 2$ ,  $H(\phi)$  is a real function, a unique property for this case. In the case of  $N = 3$ ,  $H(\phi)$  is a function of a complex variable, with support within the region  $|\phi| \leq 1$ .

Finally, we examine the scenario where  $SU(N)$  has  $N \geq 4$ . When constructing the Jacobian, we must consider its  $\mathbb{Z}_N$  invariance. According to Sannino's proposal [22], the simplest form that preserves  $\mathbb{Z}_N$  symmetry is given by

$$\mathcal{H}^{(N)}(\phi) = 1 - \lambda_2|\phi|^2 - \lambda_4|\phi|^4 + \lambda_N \text{Re } \phi^N. \quad (24)$$

It is noteworthy that the constants  $\lambda_2$ ,  $\lambda_4$ , and  $\lambda_N$  depend solely on  $N$ , and  $\lambda_N$  is expected to vanish in the large- $N$  limit, as this term breaks the  $U(1)$  symmetry that the large- $N$  theory may respect. In another study, this form is applied to the  $SU(N)$  Polyakov-Nambu-Jona-Lasinio model, and even the thermal properties of  $\lambda_2$ ,  $\lambda_4$ , and  $\lambda_N$  are investigated [23]. We subsequently take (24) as the ansatz for our model. Although higher-order terms like  $|\phi|^6$ ,  $|\phi|^8$ , ..., or  $\text{Re}\phi^{2N}$ ,  $\text{Re}\phi^{3N}$ , ... are not prohibited by invariance, we disregard these terms because their contributions are negligible. The term  $\phi^N - \phi^{*N}$  is forbidden because it violates charge conjugation symmetry.

### B. Large- $N$ limit

In this subsection, we ensure that (21) yields a massless mode in the large- $N$  limit explicitly. We consider the

fluctuation around a vacuum and obtain the correlation function of the fluctuation along the  $\theta$  direction, when  $\phi(\mathbf{x}) = l_0 e^{i\theta(\mathbf{x})/l_0}$ . We expand (24) in terms of  $l_0^N$

$$\ln \mathcal{H}^{(N)}(l_0 e^{i\theta(\mathbf{x})/l_0}) \simeq \ln \lambda - \frac{\lambda_N l_0^N}{\lambda} \left( 1 - \cos \left( \frac{N}{l_0} \theta \right) \right) \quad (25)$$

after substituting  $\phi(\mathbf{x}) = l_0 e^{i\theta(\mathbf{x})/l_0}$  into (21). Here  $\lambda \equiv 1 - \lambda_2 l_0^2 - \lambda_4 l_0^4 + \lambda_N l_0^N$  and note the upper bound condition  $l_0 < 1$ . Combining (21) and (25) and extracting the trivial constant, we obtain

$$S_{\text{YM}} = C \int d^3 \mathbf{x} \left[ \frac{1}{2} (\nabla \theta)^2 + V_{\text{YM}}(\theta) \right], \quad (26)$$

where

$$V_{\text{YM}}(\theta) \equiv \frac{m_{\text{YM}}^2 l_0^2}{N^2} \left( 1 - \cos \left( \frac{N}{l_0} \theta \right) \right), \quad (27)$$

$$m_{\text{YM}} \equiv \sqrt{\frac{e^{\beta \sigma a} \lambda_N l_0^{N-2}}{2a^2 \lambda}}. \quad (28)$$

For a small  $\theta$  fluctuation, we can focus on the vicinity of  $\theta = 0$  and generate a mass term

$$S_{\text{YM}} \simeq C \int d^3 \mathbf{x} \left[ \frac{1}{2} (\nabla \theta)^2 + \frac{m_{\text{YM}}^2}{2} \theta^2 \right]. \quad (29)$$

Based on (29), the correlation function of  $\theta(\mathbf{x})$  reads

$$\begin{aligned} \langle \theta(\mathbf{x}) \theta(0) \rangle &= \frac{\int \mathcal{D}\theta \theta(\mathbf{x}) \theta(0) e^{-S_{\text{YM}}}}{\int \mathcal{D}\theta e^{-S_{\text{YM}}}} \\ &\propto \frac{1}{|\mathbf{x}|} e^{-m_{\text{YM}} |\mathbf{x}|}. \end{aligned} \quad (30)$$

This mode gives a Yukawa-type spatial correlation with a range of  $m_{\text{YM}}^{-1}$ . Taking into account (28) and the upper bound constraint  $l_0 < 1$ , we conclude that

$$\lim_{N \rightarrow \infty} m_{\text{YM}} = 0, \quad (31)$$

namely

$$\langle \theta(\mathbf{x}) \theta(0) \rangle \propto \frac{1}{|\mathbf{x}|} \quad (32)$$

in the large- $N$  limit. This explicitly suggests that in the limit a Coulomb-type spatial correlation with an infinite range affecting the entire system, that is, the Nambu-Goldstone mode emerges. Importantly, the mode is only massless in the limit while it remains massive for finite  $N$ .

Note that the mode does not propagate in spacetime dynamically, but rather represents a static and spatial long-range correlation. This is because the imaginary-time dependence has already been integrated out and real-time evolution is not included in the model. Since the mode originated from the fluctuation along the  $\theta$  direction, it corresponds to a Nambu-Goldstone mode in a  $U(1)$ -symmetric quantum field theory.

In QCD, with three colors, the mass of this mode is approximately  $m_{\text{YM}} \simeq 2.1$  GeV. This mass (28) is calculated using a set of parameters:  $a = 0.4$  fm,  $\beta^{-1} = 400$  MeV,  $\sigma = 1.0$  GeV/fm, and  $l_0 = 0.5$ , as well as  $\lambda_2 = 6$ ,  $\lambda_4 = 3$ , and  $\lambda_N = 8$  in (23). Even though the mass of this mode is large compared to the typical mass scale of QCD, it becomes massless in the ideal large- $N$  limit.

### C. Quantum mechanical description

In this subsection, we present the one-dimensional quantum mechanical action that describes the transition between vacua. To estimate the transition rate, we must consider all possible paths connecting two vacua in the  $\phi$ -plane. However, we assume that the dominant path is along the circumference  $|\phi| = l_0$ , which reduces the problem to a one-dimensional system.

Before we discuss the properties of (26) in detail, we must ensure that quantum corrections do not violate essential symmetries. SSB due to quantum effects is a common phenomenon, as seen in the electroweak phase transition caused by quantum corrections, as derived by Coleman and Weinberg [24]. However, in the current system under study, it is demonstrated that quantum corrections up to one loop do not affect vacuum stability, and classical action suffices for physical considerations. To verify this, we add a source term to (26):  $Z_{\text{YM}}[\lambda] = \int \mathcal{D}\theta \exp[-S_{\text{YM}} + \theta \cdot \lambda]$ .<sup>4</sup> and calculate the effective potential. The generating functional of connected Green's functions

$$\begin{aligned} W_{\text{YM}}[\lambda] &\equiv -\ln Z_{\text{YM}}[\lambda] \\ &= S_{\text{YM}}[\theta_\lambda] - \theta_\lambda \cdot \lambda + \frac{1}{2} \ln \det S_{\text{YM}}^{(2)}[\theta_\lambda] \end{aligned} \quad (33)$$

is defined for the saddle point configuration  $\theta_\lambda$  that satisfies  $\partial S_{\text{YM}}/\partial\theta = \lambda$ .  $S_{\text{YM}}^{(2)}[\theta]$  represents the second functional derivative of  $S_{\text{YM}}$ . By the Legendre transformation with respect to the variable  $\lambda$ , we obtain  $\Gamma_{\text{YM}}(\langle\theta\rangle) \equiv W_{\text{YM}}[\lambda] + \langle\theta\rangle \cdot \lambda$ :

$$\begin{aligned} \Gamma_{\text{YM}}(\langle\theta\rangle) &\simeq S_{\text{YM}}(\langle\theta\rangle) + \frac{1}{2} \ln \det S_{\text{YM}}^{(2)}(\langle\theta\rangle) \\ &= S_{\text{YM}}(\langle\theta\rangle) \\ &\quad + \frac{1}{2} \text{Tr} \ln \left( -\nabla^2 + m_{\text{YM}}^2 \cos\left(\frac{N}{l_0} \langle\theta\rangle\right) \right) \\ &\simeq S(\langle\theta\rangle) + \frac{V}{2} \int \frac{d^3\mathbf{k}}{(2\pi)^3} \ln(k^2 + M_{\text{YM}}(\langle\theta\rangle)^2) \end{aligned} \quad (34)$$

up to one loop. Here  $M_{\text{YM}}(\langle\theta\rangle) \equiv m_{\text{YM}} \cos^{1/2}\left(\frac{N}{l_0} \langle\theta\rangle\right)$ . Performing the integration, we obtain the effective po-

tential:

$$\begin{aligned} V_{\text{eff}}(\langle\theta\rangle) &\simeq V_{\text{YM}}(\langle\theta\rangle) - \frac{1}{2} \frac{\Gamma(-3/2)}{(4\pi)^{3/2}} (M_{\text{YM}}(\langle\theta\rangle)^2)^{3/2} \\ &= V_{\text{YM}}(\langle\theta\rangle) - \frac{1}{12\pi} M_{\text{YM}}(\langle\theta\rangle)^3. \end{aligned} \quad (35)$$

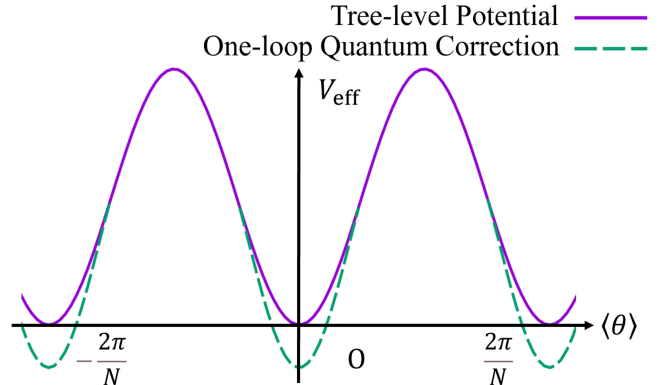


FIG. 5: The tree-level potential and the one-loop quantum correction are shown. Note that the locations of the minimum points are unchanged and the  $\mathbb{Z}_N$  symmetry is preserved.

The results shown in (35) and Fig. 5 clarify the two points: quantum corrections do not violate the  $\mathbb{Z}_N$  symmetry of the action, and the contribution from quantum corrections vanishes faster than the tree-level term in the large- $N$  limit. As long as our discussion is limited to the systems with sufficiently large  $N$ , the quantum corrections do not play a significant role. Then, we safely ignore the quantum corrections and consider this problem at the tree level going forward.

In the following, we suppose that the field  $\theta(\mathbf{x})$  has an imaginary-time dependence and treat  $\theta$  as a real scalar field on a (1+3)-dimensional Euclidean spacetime. We introduce the time derivative term with a parameter  $Z$  and define

$$S_{\text{QM}} = \frac{C}{a} \int d\tau \int_V d^3\mathbf{x} \left[ \frac{Z}{2} \left( \frac{\partial\theta}{\partial\tau} \right)^2 + \frac{1}{2} (\nabla\theta)^2 + V_{\text{YM}}(\theta) \right]. \quad (36)$$

The imaginary time formalism allows  $Z$  to be a non-trivial constant, as space and time are no longer compatible variables in this framework. For the purpose of qualitatively evaluating the nature of the action, we put  $Z = 1$  as an ansatz.

To analyze the homogeneous configuration in a finite domain, we suppose that  $\theta(\tau, \mathbf{x})$  is homogeneous with respect to the spatial coordinate  $\mathbf{x}$ :

$$S_{\text{QM}} = \frac{CV}{a} \int d\tau \left[ \frac{1}{2} \left( \frac{\partial\theta}{\partial\tau} \right)^2 + V_{\text{YM}}(\theta) \right]. \quad (37)$$

The action represents that of a quantum dynamical particle, and we interpret the vacuum-to-vacuum transition

<sup>4</sup> Here  $\theta \cdot \lambda$  is an abbreviation for  $\int_V d^3\mathbf{x} \theta(\mathbf{x}) \lambda(\mathbf{x})$

as the dynamics of some virtual particle following this action.

## V. CENTER DOMAIN VOLUME

In this section, we estimate the lifetime of a vacuum and the center domain volume based on (37). For later convenience, we define the coefficient in (37) as follows:

$$S_{\text{QM}} \equiv \int d\tau \left[ \frac{M(V, N)}{2} \left( \frac{\partial \theta}{\partial \tau} \right)^2 + \frac{V_0(V, N)}{2} \left( 1 - \cos \left( \frac{N}{l_0} \theta \right) \right) \right], \quad (38)$$

where

$$M(V, N) \equiv \frac{CV}{a} = \left( \frac{N}{a} \right)^2 V e^{-\beta \sigma a}, \quad (39)$$

$$V_0(V, N) \equiv \frac{2l_0^2 m_{\text{YM}}^2}{N^2 a} CV = \frac{V}{a^4} \frac{\lambda_N}{\lambda} l_0^N \quad (40)$$

Note that in (40) the  $N$  dependence appears in  $\lambda_N/\lambda$  and  $l_0^N$ , but the dominant contribution comes from the latter exponentiation. Although  $\lambda_N/\lambda$  is expected to vanish as  $N \rightarrow \infty$ , here we assume that the dependence is less dominant compared to  $l_0^N$  for the later numerical calculation.

The transition between two adjacent wells can occur in two ways:

1. The thermal transition: a particle with energy  $E \geq V_0(V, N)$  surmounts the potential barrier.
2. The quantum transition: a particle with energy  $E < V_0(V, N)$  tunnels through the potential barrier.

We define the transition rate from one well to the adjacent one per unit of imaginary time  $\Gamma_{\text{th}}(V, N)$  for case 1 and  $\Gamma_{\text{tun}}(V, N; E)$  for case 2. The total transition rate per unit of imaginary time  $\Gamma_{\text{tot}}(V, N)$  is given by the sum of these two rates:

$$\Gamma_{\text{tot}}(V, N) = \Gamma_{\text{th}}(V, N) + \langle \Gamma_{\text{tun}}(V, N; E) \rangle, \quad (41)$$

where  $\langle \bullet \rangle$  denotes a thermal expectation value.

### A. On the $(V^{1/3}, N)$ -plane

In this subsection, we analytically calculate the transition rates  $\Gamma_{\text{tot}}(V, N)$  and estimate the lifetime of a vacuum  $\tau_v(V, N) = 1/\Gamma_{\text{tot}}(V, N)$ .

$\Gamma_{\text{th}}(V, N)$  can be evaluated easily:

$$\Gamma_{\text{th}}(V, N) = \frac{1}{\beta} \frac{\int_{V_0}^{\infty} dE e^{-\beta E}}{\int_0^{\infty} dE e^{-\beta E}} = \frac{1}{\beta} e^{-\beta V_0(V, N)}. \quad (42)$$

Here  $1/\beta$  is a typical frequency of thermal fluctuation called *attempt frequency* in solid-state physics.

$\Gamma_{\text{tun}}(V, N; E)$  can be evaluated using penetration rate per collision  $P(V, N; E)$ , or the *Gamow factor*:

$$\Gamma_{\text{tun}}(V, N; E) = 2E \cdot P(V, N; E). \quad (43)$$

To obtain  $P(V, N; E)$ , a semi-classical estimate using the WKB approximation is sufficient:

$$P(V, N; E) = \exp \left[ -2 \int_{\theta_0}^{\frac{2\pi l_0}{N} - \theta_0} d\theta \sqrt{2M(V(\theta) - E)} \right], \quad (44)$$

where  $V(\theta_0) = E$  ( $0 \leq \theta_0 \leq \frac{l_0}{N}\pi$ ). Using the expression, the thermal average of the transition rate can be calculated:

$$\langle \Gamma_{\text{tun}}(V, N; E) \rangle = \int_0^{V_0} dE 2E \cdot P(V, N; E) e^{-\beta E}. \quad (45)$$

Combining (42) and (45), we evaluate (41) numerically using the parameter set as follows: lattice spacing  $a = 0.4$  fm, temperature  $T = 400$  MeV, string tension at zero temperature  $\sigma = 1.0$  GeV/fm,  $\lambda_N/\lambda = 7.52$  and the vacuum expectation value  $l_0 = 0.5$ . Note that here we regard  $\lambda_N/\lambda$  as approximately the constant independent of  $N$  and utilize  $\lambda_2 = 6$ ,  $\lambda_4 = 3$ , and  $\lambda_N = 8$  in (23). This approximation is made because  $\lambda_N/\lambda$  always appears as the product with  $l_0^N$ , and the  $N$  dependence of the latter is expected to be more dominant in the large- $N$  limit. Therefore, it suffices to neglect the  $N$  dependence of the former and to focus on the most significant  $N$  dependence to demonstrate the qualitative properties of the model.

The figure in Fig. 6 displays the dependence of the total transition rate  $\Gamma_{\text{tot}}$  on  $(V, N)$ . On a specific curve, the transition rate sharply decreases. The lifetime  $\tau_v$  is shown in Fig. 7. This figure exposes that the  $(V^{1/3}, N)$ -plane splits into two separate regions: the stable and unstable vacuum regions. The boundary between these two phases is a fuzzy crossover, defined by the rapid rise in lifetime. The ‘‘critical curve,’’ where the lifetime intersects 1.0 fm, is illustrated in Fig. 8 for  $T = 300$  MeV, 400 MeV, 500 MeV, and 600 MeV.

It is important to note that the crossover curves are also dependent on the lattice spacing, which is one of the parameters of the model. Considering the strong coupling approximation and the asymptotic freedom, we set the lattice spacing  $a$  to 0.4 fm, which is larger than the typical length scale of hadrons but smaller than that of the modes studied.

Our findings provide insights into the structure of center domains and domain walls in the quark-gluon plasma. In high-energy heavy-ion collision experiments, the system is divided into thousands of small center domains with different vacuum configurations. Considering that the configuration of the domain smaller than the ‘‘critical volume’’ is likely to decay, the typical lower bound of the center domain volumes corresponds to the ‘‘critical volume.’’

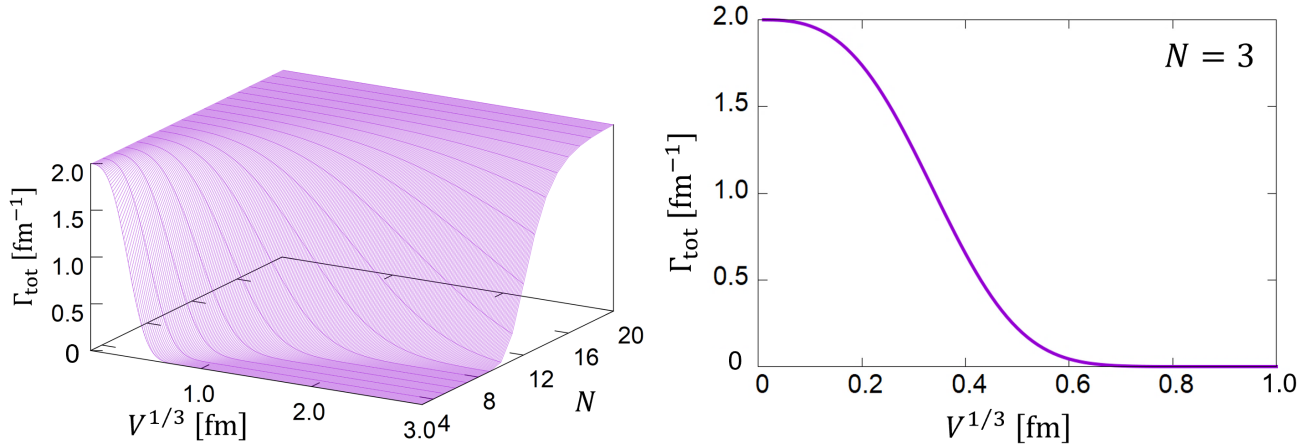


FIG. 6: The figures show the total transition rate of the vacuum as a function of  $V^{1/3}$  and  $N$  (left panel) and for  $N = 3$  (right panel). These rates were calculated using the following parameter set: lattice spacing  $a = 0.4$  fm, temperature  $T = 400$  MeV, string tension at zero temperature  $\sigma = 1.0$  GeV/fm,  $\lambda_N/\lambda = 7.52$  and the vacuum expectation value  $l_0 = 0.5$ . Here we regard  $\lambda_N/\lambda$  as the constant independent of  $N$  and utilize  $\lambda_2 = 6$ ,  $\lambda_4 = 3$ , and  $\lambda_N = 8$  in (23) because the product of the parameter  $\lambda_N/\lambda$  with  $l_0^N$  always appears, and the  $N$  dependence of the latter is expected to be more dominant in the large- $N$  limit. Therefore, it suffices to neglect the  $N$  dependence of the former and focus on extracting the most significant  $N$  dependence,  $l_0^N$ , to study the qualitative properties of the model. The saturation of the rate in the large- $N$  region indicates that the transition is primarily driven by thermal processes, rather than quantum tunnelling.

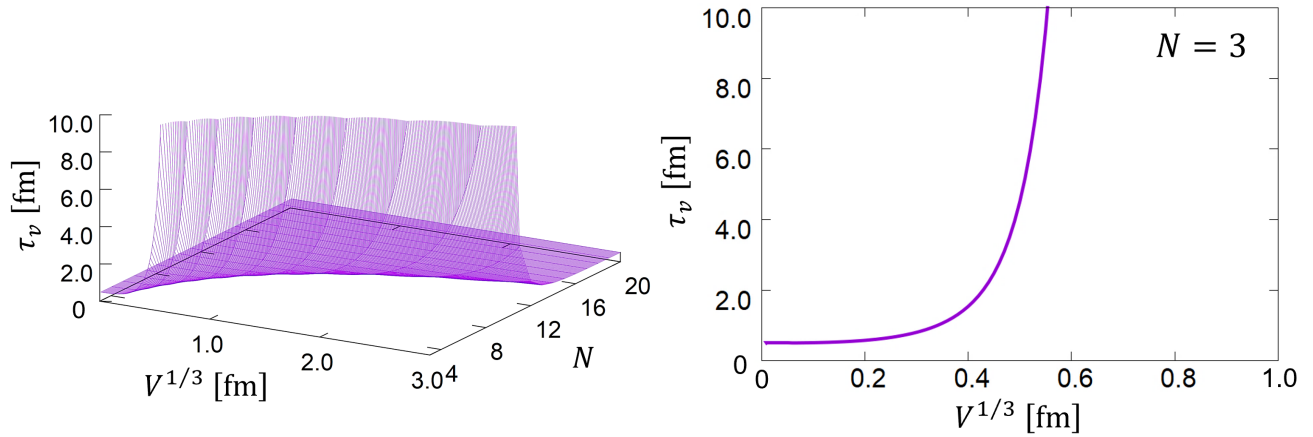


FIG. 7: The figures show the lifetime of the vacuum as a function of  $V^{1/3}$  and  $N$  (left panel) and for  $N = 3$  (right panel). These lifetimes were calculated using the same set of parameters as in Fig. 6. There is a specific line on which the lifetime sharply increases, dividing the  $(V^{1/3}, N)$  plane into two distinct regions. In the region of large  $N$  and small  $V$ , the vacuum is unstable and easily transitions to another vacuum, while in the region of small  $N$  and large  $V$ , the vacuum is stable.

### B. Extreme cases

In addition to the above results for finite  $N$  and  $V$ , we consider the vacuum stability in such extreme cases as  $V \rightarrow \infty$  and the large- $N$  limit.

In the  $V \rightarrow \infty$  limit, since both  $V_0(V, N)$  and  $M(V, N)$  diverge,

$$\lim_{V \rightarrow \infty} \Gamma_{\text{th}}(V, N) = 0. \quad (46)$$

Using  $\theta_0 = 0$  from  $\frac{V_0}{2} \left(1 - \cos\left(\frac{N}{l_0}\theta\right)\right) - E \simeq \frac{V_0}{2} \left(1 - \cos\left(\frac{N}{l_0}\theta\right)\right) = 0$  followed by  $V_0 \gg E$ , the Gamow

factor in WKB approximation can be calculated:

$$\begin{aligned} P(V, N; E) &\simeq P(V, N; 0) \\ &= \exp \left[ -2 \int_0^{\frac{2\pi l_0}{N}} d\theta \sqrt{2MV(\theta)} \right] \\ &= \exp \left[ -\frac{16\sqrt{MV_0}}{N} \right]. \end{aligned} \quad (47)$$

Thus,

$$\begin{aligned} \lim_{V \rightarrow \infty} \langle \Gamma_{\text{tun}}(V, N; E) \rangle_\beta & \\ &\simeq \lim_{V \rightarrow \infty} 2\beta P(V, N; 0) \int_0^\infty dE E e^{-\beta E} = 0. \end{aligned} \quad (48)$$

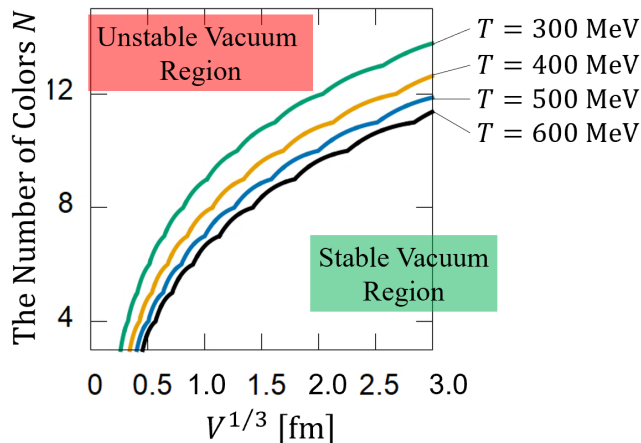


FIG. 8: The crossover transition between the unstable vacuum region and the stable vacuum region is shown for different temperatures:  $T = 300\text{MeV}$ ,  $400\text{MeV}$ ,  $500\text{MeV}$ ,  $600\text{MeV}$ . The lifetime of the vacuum lasts for 1.0 fm on the transition curves, which corresponds to the typical timescale of hadrons. Domains smaller than the transition thresholds, or unstable domains, would shrink and disappear, while those larger than the thresholds would be stabilized.

Therefore, we can say that vacua become irreducible by  $V \rightarrow \infty$ , i.e.  $\Gamma_{\text{tot}} \rightarrow 0$ . In other words, the vacuum gets stable:  $\tau_v(V, N) \rightarrow \infty$ . We derive the irreducibility using the instanton method in Appendix A.

In the large- $N$  limit,  $V_0(V, N) \rightarrow 0$  and  $M(V, N) \rightarrow \infty$  is followed by

$$\lim_{N \rightarrow \infty} \Gamma_{\text{th}}(V, N) = \frac{1}{\beta}. \quad (49)$$

and

$$\lim_{N \rightarrow \infty} \langle \Gamma_{\text{tun}}(V, N; E) \rangle = \Gamma_{\text{tun}}(E = 0) = 0 \quad (50)$$

considering  $0 < E \leq V_0$ . Therefore, the dominant contribution comes from the thermal effect rather than the tunneling. In this case, a particle is completely free from the potential, and the lifetime of the vacuum is  $\tau_v(V, N) \rightarrow \beta$ , comparable to the time scale of the thermal fluctuation.

## VI. CONCLUSION

In this paper, we investigate the non-trivial  $\mathbb{Z}_N$  configuration in the deconfinement vacuum of  $\text{SU}(N)$  Yang-Mills theory. We expand the known effective action of QCD to the  $\text{SU}(N)$  Yang-Mills theory, considering spatial dependence.

In the first section, we develop the Polyakov loop effective action for the theory with a finite number of colors. We examine the correlation function of the Polyakov loop and successfully derive the fluctuation mass as a function of the color number, based on the model. We also analyze the global symmetry structure metamorphosis in the

large- $N$  limit, focusing on the fluctuation of the Polyakov loop along its angle direction, which becomes a Nambu-Goldstone mode. This confirms that the limit changes the  $\mathbb{Z}_N$ -symmetric theory into a  $\text{U}(1)$ -symmetric theory.

In the second section, we investigate the global  $\mathbb{Z}_N$  structure in the finite-volume quark-gluon plasma. We model the global transition as a one-dimensional movement of a particle to compute the transition probability between different degenerate vacua. We consider both the thermal and the quantum effects and calculate the lifetime of a domain until it decays. Specifically, we show that the lifetime diverges in the infinite volume limit and vanishes in the large- $N$  limit.

In the last section, we study the typical volume scale of one of the center domains in the quark-gluon plasma as a function of the color number and volume. We discover that the  $(V^{1/3}, N)$ -plane can be divided into two regions: stable vacuum and unstable vacuum regions. This indicates that a center domain is stable if its volume exceeds a certain threshold, while a center domain with a volume below it is unstable. We identify the threshold as the lower bound of a stable center domain volume.

In conclusion, we provide a successful description of the  $\mathbb{Z}_N$  configuration in the deconfinement vacuum of  $\text{SU}(N)$  Yang-Mills theory.

Future work includes improving the strong coupling expansion that our model is based on, as well as expanding the effective model to include fermions and finite baryon densities. We also find it interesting and important to numerically verify our results using the lattice Monte-Carlo simulation.

## ACKNOWLEDGMENTS

H.S. is supported in part by the Grants-in-Aid for Scientific Research [19K03869] from Japan Society for the Promotion of Science.

## Appendix A: Tunnelling estimation by instanton method

In this appendix, we see that different vacua become irreducible as  $N \rightarrow \infty$  using the *instanton* method. For later convenience, we transform  $\theta \mapsto \theta - (l_0/N)\pi$  and rewrite (37):

$$\begin{aligned} S_{\text{QM}} &= \int d\eta \left[ \frac{1}{2} \left( \frac{\partial \Theta}{\partial \eta} \right)^2 + \frac{1}{G^2} (1 + \cos(G\Theta)) \right] \\ &\equiv \int d\eta \mathcal{L}_{\text{QM}}, \end{aligned} \quad (\text{A1})$$

where  $\Theta$ ,  $\eta$ , and  $G$  are dimensionless quantities:

$$\eta \equiv m_{\text{YM}} \tau \quad (\text{A2})$$

$$\Theta \equiv \sqrt{\frac{m_{\text{YM}} C V}{a}} \theta \quad (\text{A3})$$

$$G \equiv \frac{N}{l_0} \sqrt{\frac{a}{m_{\text{YM}} C V}}. \quad (\text{A4})$$

Our current goal is to estimate the quantum tunneling amplitude between the two adjacent wells, or two adjacent vacua. Supposing that  $|\mathcal{E}\rangle_+$  and  $|\mathcal{E}\rangle_-$  represent states at energy  $\mathcal{E}$  localized at  $\Theta = +\pi/G$  and  $\Theta = -\pi/G$  respectively, the amplitude of the transition in imaginary time  $T$  is written as

$$A_{+,-} = {}_{+} \langle \mathcal{E} | e^{-2T\hat{H}} | \mathcal{E} \rangle_{-} = e^{-2\mathcal{E}T} \sinh(2\Delta\mathcal{E}T). \quad (\text{A5})$$

$\Delta\mathcal{E}$  is the off-diagonal component of Hamiltonian employing the states  $\{|\mathcal{E}\rangle_+, |\mathcal{E}\rangle_-\}$  as its basis, i.e.

$$\begin{bmatrix} {}_{+} \langle \mathcal{E} | H | \mathcal{E} \rangle_{+} & {}_{+} \langle \mathcal{E} | H | \mathcal{E} \rangle_{-} \\ -{}_{-} \langle \mathcal{E} | H | \mathcal{E} \rangle_{+} & -{}_{-} \langle \mathcal{E} | H | \mathcal{E} \rangle_{-} \end{bmatrix} \equiv \begin{bmatrix} \mathcal{E} & -\Delta\mathcal{E} \\ -\Delta\mathcal{E} & \mathcal{E} \end{bmatrix}. \quad (\text{A6})$$

On the other hand, the transition amplitude can be also expressed by path integral:

$$A_{+,-}^{(1)} = \int_{\Theta(\eta_i)}^{\Theta(\eta_f)} \mathcal{D}\Theta \exp \left[ - \int_{\eta_i}^{\eta_f} d\tau \mathcal{L}_\Theta \right], \quad (\text{A7})$$

where  $\eta_f - \eta_i \equiv 2T$ . The path integral method is a powerful tool when evaluating the non-perturbative effects, where we can treat the tunneling as quantum fluctuations around the instanton between two wells.

Instanton solution  $\Theta_c(\eta)$  have already been exactly calculated in [25]:

$$\Theta_c(\eta) = \frac{2}{G} \arcsin(k \operatorname{sn}(\eta - \eta_0, k^2)), \quad (\text{A8})$$

where  $\operatorname{sn}(x, k^2)$  is the *Jacobian elliptic function* with modulus  $k \equiv \sqrt{1 - G^2\mathcal{E}/2}$  and  $\eta_0$  denotes the position of the instanton. For zero energy ( $\mathcal{E} = 0$ ), this turns to be

$$\Theta_c(\eta) = \frac{2}{G} \arcsin(\tanh(\eta - \eta_0)). \quad (\text{A9})$$

We now set  $\Theta(\eta) = \Theta_c(\eta) + \delta\Theta(\eta)$  and perform the path integral for an exponentiated quadratic form of  $\delta\Theta(\eta)$ . As shown in [25], performing the path integral over the fluctuation around the classical solution  $\bar{\theta}_c$  yields the transition amplitude

$$A_{+,-}^{(1)} = \frac{2T}{4\mathcal{K}(k')} e^{-W} e^{-2\mathcal{E}T}, \quad (\text{A10})$$

where

$$W = \frac{8}{G^2} [E(k) - k'^2 \mathcal{K}(k)]. \quad (\text{A11})$$

Here,  $\mathcal{K}(x)$  and  $E(x)$  are the *complete elliptic integrals* of the first and second kinds, respectively, and  $k'$  is defined as  $\sqrt{1 - k^2}$ .

Note that the corresponding classical trajectories include not only the single instanton configuration but also multi-instanton configurations such as instanton–anti-instanton–instanton. Therefore, the total amplitude is the sum of all the possible configurations:

$$\begin{aligned} A_{+,-} &= \sum_{m=0}^{\infty} A_{+,-}^{(2m+1)} \\ &= e^{-2\mathcal{E}T} \sinh \left( \frac{T}{2\mathcal{K}(k')} e^{-W} \right). \end{aligned} \quad (\text{A12})$$

Combining (A5) and (A12) and assuming  $\mathcal{E} \simeq 0$ , we obtain

$$\begin{aligned} \Delta\mathcal{E} &= \frac{1}{4\mathcal{K}(k')} e^{-W} \\ &\propto \exp \left[ -\frac{8}{G^2} \right] \\ &= \exp \left[ -\frac{4\sqrt{2}V}{a} \left( l_0^{N+2} e^{-\beta\sigma a} \frac{\lambda_N}{\lambda} \right)^{1/2} \right]. \end{aligned} \quad (\text{A13})$$

Therefore, as  $V \rightarrow \infty$ , we obtain

$$\begin{bmatrix} \mathcal{E} & -\Delta\mathcal{E} \\ -\Delta\mathcal{E} & \mathcal{E} \end{bmatrix} \longrightarrow \begin{bmatrix} \mathcal{E} & 0 \\ 0 & \mathcal{E} \end{bmatrix}, \quad (\text{A14})$$

which means that the Hamiltonian becomes diagonal and the different vacua become irreducible.

- 
- [1] K. G. Wilson, Confinement of quarks, *Phys. Rev. D* **10** (1974).  
[2] A. M. Polyakov, Thermal properties of gauge fields and quark liberation, *Phys. Lett. B* **72**, 477 (1978).  
[3] L. Susskind, Dynamics of spontaneous symmetry breaking in the Weinberg-Salam theory, *Phys. Rev. D* **20**, 2610 (1979).  
[4] L. G. Yaffe and B. Svetitsky, First-order phase transition in the SU(3) gauge theory at finite temperature, *Phys. Rev. D* **26** (1982).  
[5] M. Ogilvie, Effective-spin model for finite-temperature QCD, *Phys. Rev. Lett.* **52**, 1369 (1984).  
[6] A. M. Polyakov, Compact gauge fields and the infrared catastrophe, *Phys. Lett.* **59B**, 82 (1975).  
[7] B. Svetitsky and L. G. Yaffe, Critical behavior at finite-temperature confinement transitions, *Nucl. Phys. B* **210**, 423 (1982).  
[8] R. B. Potts, Some generalized order-disorder transformations, *Math. Proc. Cambridge Philos. Soc.* **48**, 106 (1952).  
[9] J. M. Drouffe, J. Jurkiewicz, and A. Krzywicki, Lattice gauge theory with Higgs matter field in the adjoint representation, *Phys. Rev. D* **29** (1984).  
[10] J. Polonyi, Phase transition from strong-coupling expansion

- sion, Phys. Lett. B **110**, 395 (1982).
- [11] F. Green and F. Karsch, SU(4) deconfining transition at strong coupling: A Monte Carlo study, Nucl. Phys. B **238**, 297 (1984).
- [12] H. Matsuoka, Deconfinement transition and the Z(N) clock model, Phys. Lett. B **140**, 223 (1984).
- [13] G. 't Hooft, A planar diagram theory for strong interactions, Nucl. Phys. B **72**, 461 (1974).
- [14] L. McLerran and R. D. Pisarski, Phases of dense quarks at large  $N_c$ , Nucl. Phys. A **796**, 83 (2007).
- [15] P. H. Damgaard and A. Patkós, Analytic results for the effective theory of thermal Polyakov loops, Phys. Lett. B **172**, 369 (1986).
- [16] M. Billó, M. Caselle, A. D'Adda, L. Magnea, and S. Panzeri, Deconfinement transition in large- $N$  lattice gauge theory, Nucl. Phys. B **435**, 172 (1995).
- [17] M. Asakawa, S. A. Bass, and B. Müller, Center domains and their phenomenological consequences, Phys. Rev. Lett. **110** (2013).
- [18] Y. Nambu, Quasiparticles and gauge invariance in the theory of superconductivity, Phys. Rev. **117**, 648 (1960).
- [19] J. Goldstone, Field theories with superconductor solutions, Nuovo Cim. **19**, 154 (1961).
- [20] F. Y. Wu, The Potts model, Rev. Mod. Phys. **54**, 235 (1982).
- [21] B. Conrey, Notes on eigenvalue distributions for the classical compact groups (Cambridge University Press, 2005) p. 111.
- [22] F. Sannino, Higher representations: Confinement and large  $N$ , Phys. Rev. D **72** (2005).
- [23] F. Buisseret and G. Lacroix, Large- $N_c$  Polyakov–Nambu–Jona-Lasinio model with explicit  $Z_{N_c}$  symmetry, Phys. Rev. D **85** (2012).
- [24] S. Coleman and E. Weinberg, Radiative corrections as the origin of spontaneous symmetry breaking, Phys. Rev. D **7**, 1888 (1973).
- [25] J.-Q. Liang and H. J. W. Müller-Kirstein, Quantum tunneling for the sine-Gordon potential: Energy band structure and Bogomolny-Fateyev relation, Phys. Rev. D **51**, 718 (1995).